

Wave–Particle Duality as Pre-Temporal Commitment Dynamics in the VERSF Framework

VERSF Theoretical Physics Program

Abstract

Wave–particle duality can be understood as a transition between reversible possibility dynamics and irreversible fact formation within the Void Energy-Regulated Space Framework (VERSF). The framework proposes a two-layer ontology: a pre-temporal relational space R of reversible distinguishability relations, and a committed layer C of irreversible records that generates physical time. Following the reconstruction programmes of Hardy and Chiribella–D'Ariano–Perinotti, the operational axioms governing R imply that the state space must admit a complex Hilbert representation. The Born rule follows from Gleason's theorem applied to the fold interface $\Phi : \mathcal{H} \rightarrow \mathcal{P}$, the entropy-triggered stochastic outcome map from pre-temporal amplitudes to committed outcomes. Wave behaviour corresponds to reversible propagation of possible commitment pathways within R ; particle detection corresponds to an irreversible crossing of Φ triggered when system–environment entanglement entropy exceeds a threshold S_{commit} linked to the causal capacity condition $\chi(L) = \rho_{\Lambda} L^4 / (\hbar c) \sim 1$. This threshold emerges independently from the Margolus–Levitin speed limit and the Bekenstein entropy bound, with equivalent reformulations appearing in causal-diamond action and Lloyd's computational bound, all converging on the same quartic structure. VERSF identifies $\rho = \rho_{\Lambda}$ (the cosmological vacuum energy density), fixing the minimal commitment cell at $\xi \approx 82 \mu\text{m}$ and substrate timescale $\tau_s \approx 0.28 \text{ ps}$. Four experimentally accessible signatures are identified: a commitment delay beyond decoherence onset in mesoscopic systems, non-Poissonian detection timing near threshold, a τ_s -scale crossover in ultrafast switching experiments, and a departure from standard Casimir scaling near $d \sim \xi$. The arrow of time arises from the accumulated ordering of irreversible commitment events rather than being postulated.

A non-technical summary for general readers is provided in Appendix A.

Table of Contents

1. Introduction
 2. Pre-Temporal Relational Space and the Derivation of Hilbert Structure
 - 2.1 Ontological Starting Point
 - 2.2 Operational Axioms on Distinguishability
 - 2.3 From Operational Structure to Convex State Space
 - 2.4 From Convex State Space to Hilbert Structure
 - 2.5 Schrödinger Evolution as Pre-Temporal Dynamics
 3. The Fold Interface: Definition, Entropy Threshold, and Commitment Events
 - 3.1 Mathematical Definition of the Fold Interface
 - 3.2 The Entropy Threshold Condition
 - 3.3 The Commitment Threshold S_{commit}
 - 3.4 The Substrate Parameter Triad and Spatial Coherence Domains
 - 3.5 Relationship to Decoherence
 4. The Born Rule from Measure Preservation
 - 4.1 The Requirement of Consistent Commitment Probabilities
 - 4.2 Derivation via Gleason's Theorem
 5. Wave Behaviour as Possibility Propagation
 6. The Double-Slit Experiment and the Quantum Eraser
 - 6.1 The Double-Slit Experiment
 - 6.2 The Quantum Eraser: Erasure as Prevention, Not Reversal
 7. The Arrow of Time and the Irreversibility of Measurement
 8. Comparison with Existing Interpretations
 - 8.1 Copenhagen Interpretation
 - 8.2 Many-Worlds Interpretation
 - 8.3 Relational Quantum Mechanics
 - 8.4 QBism
 - 8.5 Spontaneous Collapse Models (GRW/CSL)
 9. Experimental Signatures and a Toy Model
 - 9.1 Commitment Delay in Mesoscopic Systems: Toy Model
 - 9.2 Non-Poissonian Timing Statistics Near Threshold
 - 9.3 Ultrafast Switching and the τ_s Crossover
 - 9.4 Casimir Force Deviation Near ξ
 10. Discussion: Broader Implications
 - 10.1 Classical Reality as Accumulated Commitment
 - 10.2 Cosmological Implications
 - 10.3 The Mesoscopic Quantum Boundary
 - 10.4 Cross-Scale Hierarchy and the χ Invariant
 11. Conclusion
 12. References
 13. Appendix A: Summary for General Readers
 14. Appendix B: Derivation of the Quartic Capacity Measure $\chi(L)$
 15. Appendix C: Minimal Commitment Cell Lemma
-

1. Introduction

Quantum mechanics has achieved extraordinary empirical success, yet its conceptual foundations remain deeply contested. Central among these issues is wave–particle duality: quantum entities produce interference patterns characteristic of extended waves, yet individual detection events are discrete and localised, as if the same entities were point particles.

Standard quantum mechanics addresses the phenomenology through the wavefunction ψ and the measurement postulate: ψ evolves unitarily under the Schrödinger equation until a measurement triggers collapse to a definite outcome. This formalism is empirically unimpeachable, but the physical content of "collapse" is unspecified. As Bell emphasised, the word "measurement" appears as a primitive in the formalism without characterisation of what physical processes qualify [1].

Existing interpretations attempt to close this gap through different strategies. Many-worlds [2] eliminates collapse by postulating that all outcomes occur in branching universes, at the cost of an unexplained preferred basis and a contested account of probability. Hidden-variable theories [3] restore classical definiteness via additional degrees of freedom, but face constraints from Bell inequalities. Spontaneous collapse models [4] modify the Schrödinger equation with stochastic terms, introducing empirically constrained but theoretically ad hoc parameters. Relational QM [5] and QBism [6] treat measurement outcomes as relational or agent-relative facts, dissolving the collapse problem at the cost of explicit realism about the quantum state.

The Void Energy-Regulated Space Framework (VERSF) proposes a different resolution. Rather than treating spacetime, particles, or wavefunctions as primitive, VERSF begins from an ontological requirement: **physical facts must be irreversibly recorded in order for reality to constitute a sequence of distinguishable events**. From this requirement, together with operational axioms on distinguishability, the Hilbert space structure of quantum mechanics and the form of the Born rule follow as consequences.

The logical structure of the VERSF programme, and of this paper's argument, is:

```
Commitment ontology
  ↓
Fold Interface Law (BCB framework – prior VERSF work)
  ↓
Pre-temporal relational space  $R$  with operational axioms
  ↓
Complex Hilbert representation (Section 2)
  ↓
Born rule (Section 4)
```

This ordering matters. The fold interface Φ is upstream of the Hilbert space representation — it is not derived from it. The Hilbert structure and the Born rule are consequences of the axioms governing R , which are themselves grounded in the requirement that Φ must exist as a boundary between reversible possibilities and irreversible facts. A reader encountering Section 4 before

Section 3 might assume Φ is defined in terms of \mathcal{H} ; the diagram above clarifies that the logical dependence runs in the opposite direction.

This paper develops the VERSF account in detail. Section 2 derives why pre-temporal relational space must be a complex Hilbert space, via the full chain from operational distinguishability through convex state space geometry to Hilbert structure. Section 3 introduces the fold interface as a mathematically defined stochastic outcome map, gives a physically grounded entropy threshold condition with its associated substrate parameter triad (ξ, τ_s, m_s) derived in companion VERSF work [17], connects these to spatial coherence domains, and distinguishes commitment from decoherence. Section 4 derives the Born rule. Section 5 interprets wave behaviour as possibility propagation. Section 6 applies the framework to the double-slit experiment and the quantum eraser. Section 7 addresses the arrow of time. Section 8 compares VERSF with competing interpretations. Section 9 presents four experimental signatures including a toy model, the ultrafast switching crossover, and the Casimir force prediction. Section 10 discusses broader implications. Section 11 concludes.

Note on companion references [17–20, 28]. Several quantitative results in this paper draw on companion VERSF papers currently available as institutional preprints. The core derivations — the derivation of $\xi = (\hbar c / \rho \Lambda)^{1/4}$, the universality of $\chi(L)$, and the τ_s and m_s values — are now reproduced in self-contained form in Appendices B and C, making the present paper independent of those manuscripts for its central claims. Reference [28] (*The Fold Interface Law*) is cited in two load-bearing places: the fold interface geometry claim in Section 3.1 and the TPB Hilbert-space dimension result in Section 2.4. All companion papers [17–20, 28] provide fuller treatments, additional physical context, and extensions; they will be deposited as public preprints (with arXiv identifiers) to coincide with submission of this paper.

2. Pre-Temporal Relational Space and the Derivation of Hilbert Structure

2.1 Ontological Starting Point

VERSF distinguishes two fundamental ontological layers:

1. **Pre-temporal relational space R** : the structured space of distinguishable configurations that may become committed physical events, governed by reversible dynamics.
2. **Committed physical reality C** : the set of irreversible records (facts) constituting observable spacetime.

Physical time in VERSF is not a primitive container but an emergent ordering relation generated by the accumulation of irreversible commitments in C . Temporal ordering is therefore undefined within R prior to commitment.

2.2 Operational Axioms on Distinguishability

We derive the structure of R from operational axioms concerning how configurations can be distinguished. This mirrors the Hardy–Chiribella–D'Ariano–Perinotti (HCDP) programme [7, 8] but is grounded in VERSF's commitment ontology.

Let a **preparation** be any procedure that places a system into a configuration in R , and let a **test** be any procedure that produces a classical outcome from a configuration. We impose:

Axiom D1 (Tomographic Locality). The state of a composite system in R is completely determined by the joint outcome statistics of local tests on its subsystems.

Axiom D2 (Reversibility). For every admissible transformation T between configurations in R , there exists an admissible inverse T^{-1} .

Axiom D3 (Continuous Reversibility). Every pair of pure states of a system in R can be connected by a continuous one-parameter family of reversible transformations.

Axiom D4 (Finite Decomposition). Every mixed state in R decomposes as a finite convex mixture of pure states.

Axiom D5 (Ideal Measurement). For every pure state, there exists a test that identifies it with certainty without disturbing it.

These axioms characterise the operational structure of R . They are satisfied by quantum mechanics and, as shown by Hardy [7] and by Chiribella, D'Ariano, and Perinotti [8], are *not* jointly satisfied by classical probability theory (which fails D3) or by any theory over real or quaternionic Hilbert spaces without additional constraints.

2.3 From Operational Structure to Convex State Space

The set of states of a system in R — defined as equivalence classes of preparation procedures under outcome statistics — forms a **convex set** \mathcal{S} : if ρ_1 and ρ_2 are states, then $\lambda\rho_1 + (1 - \lambda)\rho_2$ is also a state for $\lambda \in [0, 1]$, corresponding to a randomised preparation. Pure states are the extreme points of \mathcal{S} .

The reversible transformations (Axiom D2) act on \mathcal{S} as a group G of bijections preserving the convex structure. Axiom D3 requires G to be a connected Lie group acting transitively on the pure states.

For a system with a finite number n of perfectly distinguishable states (Axiom D5), the convex state space \mathcal{S} is a compact convex set whose extreme points form a manifold on which G acts transitively. The dimension of this manifold determines the structure of the theory.

Classical case. If $\dim(\mathcal{S}) = n - 1$ (the simplex), the theory is classical probability theory. Reversible dynamics are permutations of pure states, and Axiom D3 fails: there is no continuous path of reversible transformations connecting distinct pure states.

Quantum case. Axiom D3 forces $\dim(\mathcal{S}) > n - 1$. For $n = 2$ (a two-state system), the unique compact convex set admitting a transitive continuous group of reversible transformations is the **3-ball** (Bloch ball), whose boundary (the Bloch sphere S^2) is the pure state manifold. This is precisely the geometry of a qubit in quantum mechanics.

2.4 From Convex State Space to Hilbert Structure

The Bloch-ball structure for $n = 2$ extends to arbitrary n by the following argument. The group G of reversible transformations, being a compact connected Lie group acting transitively on the pure state manifold, must be a compact simple Lie group. The only compact simple Lie groups that act transitively on spheres are $SO(k)$, $SU(k)$, and $Sp(k)$ (the real, complex, and quaternionic unitary groups respectively) [9].

These correspond to theories over real (\mathbb{R}), complex (\mathbb{C}), and quaternionic (\mathbb{H}) Hilbert spaces respectively.

We eliminate \mathbb{R} and \mathbb{H} on physical grounds:

- **Real Hilbert spaces** ($G = SO(k)$): Axiom D1 (tomographic locality) fails for composite systems. The state space of a bipartite real quantum system is not determined by local statistics [8], contradicting D1.
- **Quaternionic Hilbert spaces** ($G = Sp(k)$): Quaternionic quantum mechanics does not admit a consistent tensor product rule for composite systems satisfying D1 without additional structure constraints [10]. Specifically, the tensor product of quaternionic Hilbert spaces does not in general yield a quaternionic Hilbert space with the required group action.

The pre-temporal relational space R must therefore admit a representation on a **complex Hilbert space** \mathcal{H} , and reversible dynamics in R are represented by **unitary operators** on \mathcal{H} . The wavefunction $\psi \in \mathcal{H}$ represents the amplitude structure of possible commitment pathways.

Note on the derivation. The argument above follows the established reconstruction programmes of Hardy [7] and Chiribella, D'Ariano, and Perinotti [8]. VERSF's contribution is grounding these axioms in a commitment ontology — the axioms are not arbitrary operational postulates but reflect the structure required for a pre-temporal space of possible facts. The conclusion is that the VERSF axioms imply the state space must admit a complex Hilbert representation; they do not independently prove the reconstruction theorems.

Note on minimal Hilbert space dimension. The minimal local Hilbert space dimension assumed in Ticks-Per-Bit (TPB) coarse-graining analyses (\mathbb{C}^4) is argued in companion work [28] to follow from the fold interface structure. The counting argument is as follows: each minimal commitment cell is argued in [28] to support (i) two orthogonal pre-commitment amplitude

configurations, corresponding to the system being in one of two distinguishable pre-record states, and (ii) two orthogonal post-commitment configurations, corresponding to the two possible committed records. This gives $2 \times 2 = 4$ dimensions as the minimal on-site Hilbert space consistent with a single binary commitment event. This connection is developed in [28]; the present paper adopts it as a working assumption for companion TPB analyses.

2.5 Schrödinger Evolution as Pre-Temporal Dynamics

A continuous one-parameter group of unitary operators $\{U(s)\}$ on \mathcal{H} satisfying Stone's theorem has the form:

$$U(s) = e^{(-iHs/\hbar)}$$

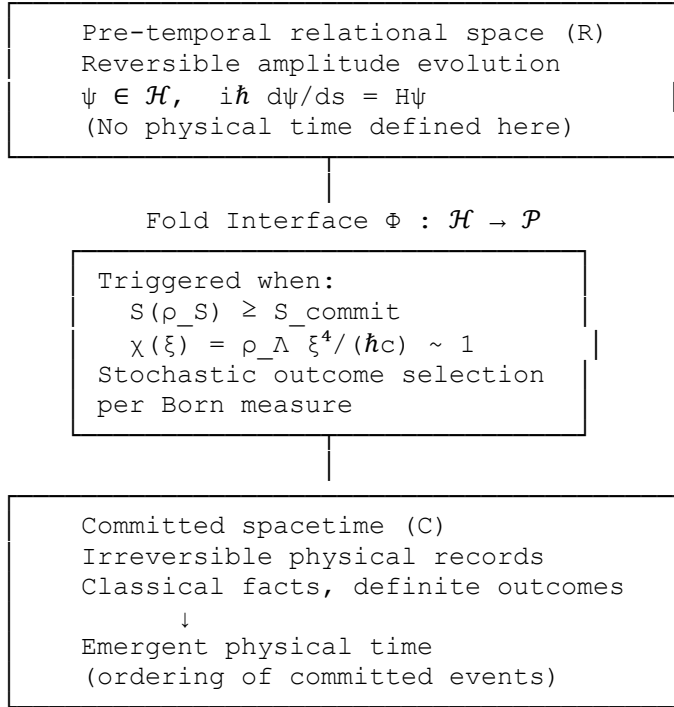
where H is a self-adjoint operator on \mathcal{H} . The evolution equation for $\psi \in \mathcal{H}$ is:

$$i\hbar \, d\psi/ds = H\psi$$

This is the Schrödinger equation. Within VERSF, this equation describes the reversible evolution of commitment pathway amplitudes in R . The parameter s is a **formal relational ordering parameter** on the amplitude structure of R — it labels the ordering of reversible configurations and is not directly observable prior to commitment. It should not be read as a physical time variable. Physical time is not a primitive of the framework; it emerges only from the accumulation of commitment events described in Section 3. The parameter s plays a proto-temporal role in the sense that it orders amplitude configurations, but the identification of any value of s with a physical moment in time requires a committed record to exist, which by definition it does not within R .

3. The Fold Interface: Definition, Entropy Threshold, and Commitment Events

The following diagram summarises the ontological structure this section develops. It shows the two-layer architecture of VERSF, the role of Φ as the boundary between them, and the physical conditions that determine when Φ is triggered:



3.1 Mathematical Definition of the Fold Interface

The **fold interface** Φ is the map from pre-temporal Hilbert space to classical probability space:

$$\Phi : \mathcal{H} \rightarrow \mathcal{P}$$

where \mathcal{P} is the classical probability simplex over committed outcomes. Φ is not a unitary map (it is not reversible) and not a linear map (it selects one outcome from a superposition). It is a physically triggered, entropy-conditioned map that operates when the system–environment state satisfies the commitment criterion defined below.

Φ formalises what collapse models posit informally: it is the physical process by which a possibility becomes a fact. Formally, Φ acts as a **stochastic outcome map**: conditioned on the entropy threshold being crossed, it selects one outcome from the amplitude distribution according to the Born measure and writes an irreversible record in C . It is not a dynamical law governing the continuous evolution of ψ — that is the Schrödinger equation — but the discrete, entropy-triggered transition from the reversible pre-temporal layer R to the committed layer C . In quantum instrument language, Φ corresponds to the instrument element triggered when the entropy threshold condition is satisfied.

The fold interface is not an independent postulate. Companion VERSF work — specifically the Fold Interface Law analysis within the BCB programme — argues for the existence of such an interface from the requirement that reversible distinguishability relations must transition into irreversible physical records in any universe capable of supporting stable facts. This transition boundary is developed in *The Fold Interface Law* [28], which presents a structural argument

from the BCB framework together with the necessity of a commitment barrier separating reversible pre-fact dynamics from committed spacetime records. The present paper therefore treats Φ as the operational manifestation of that boundary, focusing on the entropy and causal capacity conditions that determine when it is triggered in physical systems. The logical position of Φ within the VERSF programme is clarified in Section 1.

The fold interface is characterised by three physical scales — collectively the **substrate parameter triad** — that determine where and when commitment operates. These are derived in companion VERSF work [17, 18]. Papers [19] and [20] together establish the foundational result that underpins all three parameters: the dimensionless parameter $\chi(L) = \rho L^4/(\hbar c)$ is a *universal* measure of the physical capacity of a bounded causal region, derivable from quantum mechanics, thermodynamics, causal geometry, and information theory independently of any particular framework. VERSF's specific contribution is a single physical identification — that the energy density governing spacetime substrate dynamics is the cosmological vacuum energy density ρ_Λ . Once that identification is made, the scale at which $\chi = 1$ is fixed by universal physics alone.

Direct microscopic interpretation. Paper [20] derives $\chi(L)$ from four minimal postulates: finite degrees of freedom in any bounded region (P1); minimum action cost \hbar per irreversible update (P2, motivated by the Margolus–Levitin bound and the requirement of state orthogonalisation); causal coordination time $T(L) \sim L/c$ (P3); and homogeneous mean energy density ρ (P4). From these:

$$\text{total action available in region} = \rho L^3 \cdot (L/c) = \rho L^4/c$$

Dividing by the minimum action per irreversible event (\hbar):

$$\chi(L) = \rho L^4/(\hbar c) = (\text{total causal action budget}) / (\text{minimum action per irreversible event})$$

This is the **commitment capacity** of the region: the maximum number of distinguishable irreversible events it can support in one light-crossing time. It is not dimensional analysis — it is a ratio of two physically defined quantities with direct operational meaning [20].

Two independent physical routes and two reformulations. Two genuinely independent physical routes converge on the quartic capacity structure: a quantum speed-limit argument based on the Margolus–Levitin bound, and a thermodynamic entropy-capacity argument based on the Bekenstein limit. The causal-diamond action and Lloyd computational bound provide equivalent reformulations of the same capacity measure — they recover the same quartic from different starting languages but do not constitute logically independent derivations. This distinction is made explicit in Appendix B.

- **Margolus–Levitin throughput** (primary): a region of energy $E \sim \rho L^3$ can complete at most $N \sim E \cdot (L/c)/\hbar \sim \rho L^4/(\hbar c)$ distinguishable quantum transitions per causal crossing time
- **Bekenstein entropy bound** (primary): $S_{\text{max}} \sim \rho L^4/(\hbar c)$ for a region of energy $E \sim \rho L^3$ and radius L ; requiring $S_{\text{max}} \geq k_B \ln 2$ per record yields the same threshold

- **Causal-diamond action** (reformulation): a causal diamond of size L contains action $\mathcal{S}_{\text{cell}} \sim \rho L^4/c$; $\chi = \mathcal{S}_{\text{cell}}/\hbar$ is the action expressed in units of \hbar
- **Lloyd's computational bound** [20] (reformulation): the maximum number of logical operations a system of energy E can perform in time t is $N_{\text{ops}} \sim Et/\hbar$; for a causal region, $N_{\text{ops}} \sim \rho L^4/(\hbar c) = \chi(L)$

The ML and Bekenstein derivations are logically independent — one invokes the energy-time uncertainty relation and orthogonality; the other invokes only a thermodynamic entropy bound and a one-bit record condition. Their convergence on the same $\chi \sim 1$ threshold is non-trivial: the quantum speed limit and the thermodynamic entropy capacity limit coincide at the same causal scale [19, 20].

Four parallel threshold interpretations. At $\chi(\xi) = 1$, all four measures simultaneously reach their minimum threshold within one causal crossing time [20]:

Measure	Threshold condition
Causal action budget	$\mathcal{S}_{\text{cell}} = \hbar$ (one quantum of action)
Distinguishable quantum transitions	$N_{\text{ML}} \sim 1$
Entropy capacity	$S_{\text{max}} \sim k_{\text{B}} \ln 2$ (one bit)
Logical operations	$N_{\text{ops}} \sim 1$

These are physically distinct but mathematically equivalent — precisely what one expects of a fundamental capacity threshold rather than a limit specific to one domain [20].

Why the quartic specifically. Paper [20] identifies three structural criteria that uniquely select the quartic from among all dimensionless combinations constructible from ρ , L , \hbar , and c : extensivity (χ scales as volume $\propto L^3$ at fixed ρ), G-independence (the two primary derivations make no reference to gravity), and Planck normalisation ($\chi = 1$ at the Planck density ρ_{P} , marking the quantum gravity threshold). Among admissible combinations, $\rho L^4/\hbar c$ is the only one satisfying all three simultaneously.

Cross-scale validation. Reference [20] demonstrates that the same $\chi(L)$ yields structurally consistent results across 120 orders of magnitude: at a Schwarzschild black hole horizon, $\chi(R) \sim R^2/L_{\text{P}}^2 \sim S_{\text{BH}}$ (reproducing the Bekenstein–Hawking entropy up to numerical factors, supported by Bousso's covariant entropy bound and Jacobson's thermodynamic derivation of general relativity); at the cosmological horizon, $\chi(R_{\text{H}}) \sim 10^{122}$, coinciding with the horizon entropy, Lloyd's estimate of the universe's total computational capacity, and the Planck– Λ hierarchy. The VERSF coherence scale ξ sits between these extremes as the threshold at which the vacuum first becomes capable of classical fact formation — the smallest end of the hierarchy.

- **Coherence length** $\xi \approx 8.2 \times 10^{-5} \text{ m}$ ($\approx 82 \mu\text{m}$): the spatial scale defining the **minimal commitment cell** — the smallest spacetime region capable of completing one irreversible record within its own causal horizon. Fixed by:

$$\chi(\xi) = \rho_{\Lambda} \xi^4 / (\hbar c) = 1$$

A Minimal Commitment Cell Lemma in [18] unifies all four derivations: ξ is the unique length at which energetic self-consistency, causal completion, minimum action budget, and record-formation entropy capacity are simultaneously satisfied.

- **Substrate relaxation timescale** $\tau_s = \xi/c \approx 0.28$ ps: the causal crossing time of the minimal commitment cell — the time available to complete one irreversible record before causal separation fragments the cell [18]. It is the internal clock of the minimal commitment cell, not an inserted parameter.
- **Effective inertial scale** $m_s = \hbar/(c\xi) \approx 4 \times 10^{-39}$ kg: the effective inertial parameter associated with substrate disturbances at the coherence boundary, measuring the substrate's resistance to change and the source of the finite response time τ_s .

All three parameters derive from the single cosmological input $\rho_\Lambda \approx 6.9 \times 10^{-10}$ J/m³ without free parameters. Reference [17] shows the triad accounts for the effective mass of empty space, galactic rotation dynamics, and the cosmological constant. Reference [18] establishes that substituting the Friedmann equation into the definition of ξ yields an exact identity:

$$\xi = (8\pi/3)^{1/4} \cdot \sqrt{(L_P \cdot c/H_0)}$$

fixing the midpoint relation between ξ and the Planck and Hubble scales as a derived consequence of Friedmann cosmology, not a numerical coincidence. This identity — which places ξ at the geometric mean of the Planck length and the Hubble radius up to the order-unity Friedmann coefficient — is proved in Appendix C.6 and represents the deepest structural justification for the coherence scale.

3.2 The Entropy Threshold Condition

For a system S interacting with environment E in a joint pure state $|\Psi\rangle_{SE} \in \mathcal{H}_S \otimes \mathcal{H}_E$, define the reduced density matrix of the system:

$$\rho_S = \text{Tr}_E(|\Psi\rangle\langle\Psi|_{SE})$$

The **von Neumann entropy** of the system relative to its environment is:

$$S(\rho_S) = -\text{Tr}(\rho_S \log \rho_S)$$

This quantity measures the degree to which the system and environment have become entangled. $S(\rho_S) = 0$ corresponds to a pure system state (no entanglement, no decoherence); $S(\rho_S) = \log d$ (where $d = \dim \mathcal{H}_S$) corresponds to maximal entanglement.

The system partition is defined operationally: S consists of the degrees of freedom whose commitment record is to be produced (e.g. the position degree of freedom of the electron at the detector), and E consists of all environmental degrees of freedom entangled with S during interaction.

Commitment criterion. The fold interface Φ is triggered — a commitment event occurs — when:

$$S(\rho_S) \geq S_{\text{commit}}$$

where S_{commit} is the critical entropy threshold for fact formation, discussed in Section 3.3.

A related formulation used in earlier VERSF work [17] expresses commitment in terms of record-formation dynamics: coherence between possible commitment pathways is maintained only while *both* conditions hold simultaneously:

$$\Delta S_{\text{env}} < S_{\text{commit}} \text{ AND } t_{\text{record}} < \tau_s$$

The precise mapping between this dynamical formulation and the entropy threshold criterion $S(\rho_S) \geq S_{\text{commit}}$ has not yet been derived within a single microscopic framework. This is a genuine theoretical gap, not merely a notational difference: in principle, a system could satisfy $S(\rho_S) \geq S_{\text{commit}}$ while $t_{\text{record}} < \tau_s$ (sufficient entanglement established but insufficient causal time elapsed), or conversely $t_{\text{record}} \geq \tau_s$ while $S(\rho_S) < S_{\text{commit}}$ (sufficient time elapsed but insufficient entanglement accumulated). What happens at these boundary cases — whether the two conditions can be independently satisfied or whether the BCB framework implies they are always jointly approached — has not been determined. In the present paper the two are therefore treated as complementary operational characterisations of the same transition without claiming formal equivalence: one expressed in terms of the von Neumann entropy of the reduced state, the other in terms of the elapsed record-formation time relative to the substrate relaxation timescale. In practice they are tightly coupled for the physical systems considered — the rate at which entanglement entropy accumulates in ρ_S determines how rapidly t_{record} approaches τ_s — and both point to the same physical boundary. Establishing the formal relationship between them is an identified open problem for the BCB programme. The timescale $\tau_s \approx 0.28$ ps sets a characteristic window within which coherence can in principle be maintained or restored, as explored experimentally in Section 9.3.

3.3 The Commitment Threshold S_{commit}

The threshold S_{commit} is the minimum von Neumann entropy that the system–environment entangled state must achieve for an irreversible, distinguishable physical record to exist.

S_{commit} represents the local manifestation of the global causal-capacity condition $\chi(L) \approx 1$. The χ threshold determines when a causal region — a minimal causal-capacity cell — can support irreversible record formation at all; S_{commit} specifies the entanglement entropy required for that capacity to be realised in a particular system–environment interaction. The two conditions address different levels of description — causal geometry versus local quantum dynamics — and their precise formal equivalence within a single microscopic framework remains to be derived, as noted in conclusion point 4.

We do not identify S_{commit} with the Landauer bound $k_B \ln 2$ per bit [11]. The Landauer bound is the minimum thermodynamic energy cost of **erasing** one bit of classical information —

a statement about thermodynamic work in the committed layer C . The commitment threshold is a statement about the minimum entanglement entropy required in R for a committed record to be producible in C . These are distinct physical conditions.

Within the VERSF Bit Conservation and Balance (BCB) framework, a committed record of N distinguishable bits requires that the system has established at least N distinguishable correlations with environmental degrees of freedom. Each such correlation contributes at least $k_B \ln 2$ to the von Neumann entropy of the reduced state (since the minimum entropy of a two-outcome correlation is $\ln 2$). Therefore:

$$S_{\text{commit}} \geq N \cdot k_B \ln 2$$

This lower bound is independently supported by the Bekenstein entropy capacity of a substrate cell of size L [18, 19]. The maximum entropy available to a cell of energy $E \sim \rho L^3$ confined to region L is $S_{\text{max}}(L) \sim \rho L^4 / (\hbar c)$. Requiring $S_{\text{max}} \geq k_B \ln 2$ for at least one-bit record formation recovers the same quartic condition $\rho L^4 \gtrsim \hbar c$ that defines the minimal commitment cell. Crucially, the Bekenstein derivation of this threshold is genuinely independent of the Margolus-Levitin throughput derivation: it invokes only an entropy bound and a one-bit record condition, with no reference to the energy-time uncertainty relation or quantum orthogonality [19]. Their convergence on the same $\chi \sim 1$ threshold is non-trivial — it says the quantum speed limit and the thermodynamic entropy capacity limit coincide at the same causal scale. For present purposes, S_{commit} remains a symbolic threshold constrained by this lower bound; its precise value for specific physical systems is a further prediction of the BCB framework, to be developed in separate work.

Commitment events correspond to the minimal irreversible records required for fact formation. The stronger notion of realised classical information used in Ticks-Per-Bit (TPB) coarse-graining analyses imposes additional stability and correlation conditions beyond irreversibility alone — local readability, dynamical stability, and correlation support with a classical environment. Realised classical information therefore forms a subset of committed records; the commitment threshold S_{commit} is a necessary but not sufficient condition for the stronger classical information criterion.

3.4 The Substrate Parameter Triad and Spatial Coherence Domains

Section 3.1 introduced the substrate parameter triad (ξ, τ_s, m_s) and the $\chi(L)$ order parameter. This section explains how these parameters govern the spatial structure of coherence domains in committed spacetime and reconciles the triad with earlier VERSF references to a characteristic "hair-width" coherence scale.

The $\chi(L)$ order parameter and coherence domains. As established in [19] on grounds independent of VERSF, the dimensionless ratio:

$$\chi(L) = \rho_{\Lambda} L^4 / (\hbar c)$$

is the universal **causal capacity parameter** — the fundamental measure of what a bounded spacetime region can do. Its physical interpretation [19]:

- $\chi(L) < 1$: domain action insufficient; cosmological vacuum dominates; irreversible commitment dynamically underpowered within one causal cell
- $\chi(L) = 1$: crossover; defines ξ — the minimal commitment cell
- $\chi(L) > 1$: domain self-sustaining; domains of this size are composites of ξ -cells, each capable of independent record formation

A **spatial coherence domain** is therefore the region of committed spacetime C within which $\chi(L) < 1$ locally — that is, regions whose effective causal capacity satisfies $\chi(L) < 1$, where environmental entanglement entropy remains below the commitment threshold $S(\rho_S) < S_{\text{commit}}$. The connection between the local $\chi(L)$ condition and the entanglement entropy condition is physically plausible (both express the requirement that a region lacks sufficient causal capacity for irreversible record formation) but has not yet been derived within this paper from a common microscopic theory; it is noted here as a structural link to be made rigorous in future work.

Derivation of ξ . From $\rho_\Lambda \approx 6.9 \times 10^{-10} \text{ J/m}^3$ [18]:

$$\xi = (\hbar c / \rho_\Lambda)^{1/4} \approx 8.2 \times 10^{-5} \text{ m} (\approx 82 \mu\text{m})$$

This value is not a free parameter: it is fixed by \hbar , c , and the single cosmological measurement ρ_Λ . The uncertainty is approximately $\pm 20\%$ from modeling assumptions and the current Hubble tension.

Uniqueness. Reference [18] establishes that ξ is the unique minimal commitment scale singled out by the present causal-capacity construction: domains smaller than ξ ($\chi < 1$) cannot complete one irreversible commitment within their causal horizon; domains larger than ξ ($\chi > 1$) are composite aggregates of ξ -cells, not fundamental units of fact formation. The coherence scale is therefore the irreducible minimal unit within this construction.

The coherence domain as an environmental quantity. In ordinary macroscopic environments, the coherence domain extends to approximately $\xi \approx 82 \mu\text{m}$, because thermal and electromagnetic coupling rapidly drives entropy production above S_{commit} at larger scales. In carefully isolated systems — interferometers, superconducting circuits, cold-atom condensates — environmental coupling is suppressed, and the coherence domain extends to macroscopic distances, consistent with observation. The coherence domain length ℓ_{coh} scales as:

$$\ell_{\text{coh}} \sim v \cdot S_{\text{commit}} / \dot{S}_{\text{env}}$$

where v is the characteristic amplitude propagation speed and \dot{S}_{env} is the environmental entropy production rate. The scale ξ represents ℓ_{coh} in the specific case $\dot{S}_{\text{env}} = \rho_\Lambda c / S_{\text{commit}}$ — the case where the cosmological vacuum sets the entropy production floor.

Ontological clarification. The substrate parameter triad characterises the physical properties of committed spacetime C — specifically the properties of the fold interface Φ as it manifests in physical space. The triad does not introduce additional structure into pre-temporal relational space R . This is important: the Hilbert space structure of R is fixed by the operational axioms D1–D5; the parameters ξ , τ_s , and m_s describe the physical scales at which Φ operates within C . The coherence domain is therefore the region within C where Φ has not yet been triggered — where the committed layer still permits reversible amplitude dynamics from R to determine physical outcomes.

3.5 Relationship to Decoherence

Standard decoherence theory [12] describes how entanglement with environmental degrees of freedom suppresses off-diagonal terms in the system's reduced density matrix, effectively selecting a preferred pointer basis. Decoherence does not, however, produce definite outcomes in standard quantum mechanics: it produces an improper mixture that remains formally a superposition.

Within VERSF, decoherence and commitment are related but distinct:

Process	Condition	Timescale	Physical effect
Decoherence onset	Off-diagonal terms of ρ_S suppressed	$\tau_D \sim 1/(g\sqrt{N})$	Interference terms eliminated
Commitment	Associated with crossing the VERSF commitment boundary; characterised phenomenologically by $S(\rho_S)$ approaching S_{commit} and t_{record} approaching τ_s — exact microscopic relation between these criteria remains to be derived	$\tau_C \gtrsim \tau_D$ (coinciding when $\alpha \rightarrow 0$)	Irreversible record produced; Φ triggered

Decoherence is a necessary but not sufficient condition for commitment. A system may decohere (lose interference) while $S(\rho_S)$ remains below S_{commit} if the entanglement is distributed diffusely across a large environment without concentrating sufficient entropy in the system partition. Commitment additionally requires that the entanglement entropy of the system–environment partition reach the threshold for irreversible record formation.

4. The Born Rule from Measure Preservation

4.1 The Requirement of Consistent Commitment Probabilities

A complete account of quantum mechanics must derive the Born rule — the prescription that the probability of outcome $|a_n\rangle$ given state $|\psi\rangle$ is $|\langle a_n|\psi\rangle|^2$.

Within VERSF, the Born rule emerges from requiring that Φ define a **consistent probability measure** over committed outcomes.

4.2 Derivation via Gleason's Theorem

Let $|\psi\rangle = \sum_n c_n |a_n\rangle$ be the pre-commitment amplitude structure in \mathcal{H} , where $\{|a_n\rangle\}$ is the orthonormal basis of committed outcomes. The fold interface Φ must assign probabilities $P(a_n)$ to committed outcomes. We impose:

Axiom B1 (Normalisation). Φ defines a probability measure: $\sum_n P(a_n) = 1$.

Axiom B2 (Non-contextuality). $P(a_n)$ depends only on the projection $\hat{P}_n = |a_n\rangle\langle a_n|$ and the state $|\psi\rangle$, not on the choice of other outcomes in the measurement context.

Note on Axiom B2. Non-contextuality is not a trivial assumption. It requires that the probability Φ assigns to outcome a_n is independent of which other outcomes are included in the measurement partition — a structural constraint on how the fold interface maps pre-temporal amplitudes to committed probabilities. Within the present paper, B2 is adopted as a structural assumption on commitment probabilities, but a partial physical argument from the commitment ontology is available. In pre-temporal relational space R , each possible commitment pathway evolves independently under unitary dynamics before any commitment event occurs. The amplitude for pathway $|a_n\rangle$ is independently constituted from the amplitude for any other pathway $|a_m\rangle$: no causal connection between pathways exists within R prior to the commitment event, since causal connections in R are reversible distinguishability relations, not committed facts. There is therefore no mechanism by which the availability of alternative pathways $|a_m\rangle \neq |a_n\rangle$ could influence the amplitude structure of $|a_n\rangle$ or the probability Φ assigns to it. This causal independence of pre-commitment pathways provides a physical motivation for B2, though a rigorous derivation from the VERSF axioms — establishing that the fold interface cannot access partition-level information about co-available pathways — remains for future work.

Axiom B3 (Continuity). $P(a_n)$ varies continuously with $|\psi\rangle$.

These conditions define a **frame function** on the closed subspaces of \mathcal{H} in the sense of Gleason [13]. Gleason's theorem states that for $\dim \mathcal{H} \geq 3$, the only frame function satisfying B1–B3 is:

$$P(a_n) = \langle \psi | \hat{P}_n | \psi \rangle = |\langle a_n | \psi \rangle|^2$$

This is the Born rule. Within VERSF, the Born rule is a consequence of requiring that Φ be a physically consistent probability measure on the Hilbert space of pre-temporal amplitudes. It is derived, not postulated.

Note on $\dim \mathcal{H} = 2$. The present derivation is rigorous for $\dim \mathcal{H} \geq 3$. For two-dimensional systems (qubits), Gleason's theorem does not apply directly. Extension to the qubit case can be obtained by embedding the two-dimensional system into a composite system of dimension ≥ 3 via the VERSF composite system rules, so that the Gleason argument applies to the larger space and the qubit probabilities are recovered by marginalisation. An alternative route via decision-

theoretic arguments [14] is available but not pursued here. A dedicated treatment of the two-dimensional case within the VERSF ontology is deferred to future work.

5. Wave Behaviour as Possibility Propagation

Before a commitment event occurs, the system evolves unitarily in R . The amplitude structure ψ propagates across possible commitment pathways according to the Schrödinger equation.

Interference arises from the interaction of amplitudes across different pathway branches: regions where pathway amplitudes reinforce correspond to more probable commitment outcomes; regions of destructive interference correspond to suppressed outcomes.

This is not a physical oscillation of a field in spacetime. The quantum wavefunction encodes the structure of possible commitments within R — a domain in which physical time is not yet defined. It should be clearly distinguished from classical wave phenomena:

Phenomenon	Ontological layer	Physical character
Classical waves (EM, acoustic)	Committed layer C	Real oscillations of physical fields in spacetime
Quantum wavefunction ψ	Pre-temporal space R	Amplitude structure of possible commitment pathways
Particle detection	Fold interface Φ	Irreversible commitment; physical record produced

Classical waves — electromagnetic radiation, sound, water waves — are fully committed physical processes. They represent real oscillations of fields or media in spacetime, carry energy and momentum, and are described by classical dynamical equations such as Maxwell's equations. They presuppose an already-formed spacetime and belong entirely to C . The apparent similarity in terminology (both are called "waves") reflects a shared mathematical description — superposition of amplitudes — but a fundamentally different ontological status.

6. The Double-Slit Experiment and the Quantum Eraser

6.1 The Double-Slit Experiment

The double-slit experiment illustrates the VERSF commitment framework concisely.

Setup. An electron is emitted towards a barrier with two slits. A detector screen records impact positions.

VERSF account:

1. **Possibility propagation.** The amplitude structure $\psi \in \mathcal{H}$ evolves unitarily in R . Possible commitment pathways extend through both slits. No physical electron splits or travels simultaneously through two slits; the amplitude structure — encoding possible commitments — evolves through both pathway branches.
2. **Interference.** Amplitudes from the two slit branches interfere within R under unitary evolution, producing a structured distribution $\psi(x)$ across the detector plane.
3. **Commitment.** When the system–environment entanglement entropy $S(\rho_S)$ reaches S_{commit} at a detector location, a commitment event is triggered. Φ maps $|\psi\rangle$ to a definite outcome: a localised detection record at position x .
4. **Statistical reconstruction.** Repeated commitment events reconstruct the interference pattern $|\psi(x)|^2$ statistically, as required by the Born rule.

Which-path information. If a which-path detector is inserted, it entangles with the electron's path degree of freedom. This entanglement increases $S(\rho_S)$ — relative to the path partition — to S_{commit} before the electron reaches the screen. A commitment event occurs at the which-path detector, producing an irreversible record of the path. The amplitude structure ψ at the screen then carries no cross-slit coherence, and the interference pattern is destroyed. This is not because the electron "knows" it is observed, but because an earlier commitment event has already produced an irreversible fact that fixes the path degree of freedom.

6.2 The Quantum Eraser: Erasure as Prevention, Not Reversal

The quantum eraser experiment appears to allow interference patterns to be "restored" after which-path information has been acquired. In standard quantum mechanics, this is correctly described through conditional statistics on an entangled idler, but the physical mechanism — what is actually happening to the substrate — is left unspecified. The VERSF framework provides this mechanism.

Standard formalism. Consider the joint state after double-slit passage with an entangled idler particle I carrying which-path information:

$$|\Psi\rangle = (|L\rangle_S |I_L\rangle_I + |R\rangle_S |I_R\rangle_I) / \sqrt{2}$$

where $\langle I_L | I_R \rangle = 0$ (orthogonal idler states encode the path). Tracing over the idler gives a mixed reduced state for the signal — no interference pattern in unconditional statistics.

Measuring the idler in a rotated basis that does not distinguish path — $|I_+\rangle = (|I_L\rangle + |I_R\rangle) / \sqrt{2}$ — yields conditioned signal states that exhibit full interference fringes. No information propagates backward in time; the delayed-choice variant simply selects which joint correlations are analysed.

VERSF mechanism. As a phenomenological representation of coherence overlap, denote the effective substrate disturbance modes associated with the two path alternatives as $\Phi_L(x, t)$ and $\Phi_R(x, t)$. These are not yet derived from the full VERSF substrate action; they represent the amplitude structures corresponding to the two possible commitment pathways in pre-temporal space. Interference requires the coherence overlap to remain non-zero:

$$C(t) = \int \Phi_L(x,t) \Phi_R^*(x,t) d^3x \neq 0$$

In the VERSF framework, this overlap is preserved only while both $S(\rho_S) < S_{\text{commit}}$ and $t_{\text{record}} < \tau_s$. When which-path information becomes physically stabilised in the idler degrees of freedom ($S(\rho_S) \geq S_{\text{commit}}$), the substrate disturbances decohere: $C(t) \rightarrow 0$.

The critical insight is that in a quantum eraser, **no stable, path-distinguishing record is ever formed in the relevant degrees of freedom**. Measuring the idler in the erasing basis does not undo a committed record — it reveals that no such record was stabilised in the first place. The substrate coherence was preserved throughout; coincidence conditioning then selects the joint outcomes corresponding to coherent superpositions. This is entirely forward-causal: nothing propagates backward in time.

As a **phenomenological ansatz** for the decay of substrate coherence under which-path coupling — pending derivation from the full VERSF substrate action — the coherence overlap is modelled as decaying exponentially:

$$C(t) = C(0) \cdot \exp(-\Gamma t / \tau_s)$$

where Γ is a dimensionless parameter capturing the rate of which-path entanglement accumulation relative to the intrinsic substrate timescale τ_s — so that $\Gamma t / \tau_s$ is the dimensionless accumulated coupling. $\Gamma = 0$ corresponds to no which-path coupling (full coherence preserved); $\Gamma \sim 1$ corresponds to coupling on the scale of τ_s itself. The substrate relaxation timescale $\tau_s = \xi/c$ sets the natural unit against which the coupling rate is measured. This exponential form is the minimal smooth decay ansatz consistent with (i) $C \rightarrow 0$ as entanglement grows, (ii) a characteristic timescale set by τ_s , and (iii) recovery of full coherence ($C = C(0)$) at $t = 0$. It is not derived from a microscopic substrate model; the functional form and the connection between Γ and microscopic parameters await the substrate-action calculation. The observable fringe visibility under this ansatz is:

$$V = |C(t_{\text{detect}})| / C(0) = \exp(-\Gamma \cdot t_{\text{detect}} / \tau_s)$$

In the limit $t_{\text{detect}} \ll \tau_s$, the VERSF correction becomes negligible — the exponential factor approaches unity, $\Gamma \cdot t_{\text{detect}} / \tau_s \rightarrow 0$ — so the standard quantum-mechanical prediction is effectively recovered to leading order. Deviations are predicted when $t_{\text{detect}} \sim \tau_s$. The τ_s -scale crossover is a distinctive VERSF prediction, not a restatement of standard quantum mechanics; it is developed as an experimental signature in Section 9.3.

7. The Arrow of Time and the Irreversibility of Measurement

A persistent difficulty in quantum foundations is explaining the asymmetry between unitary evolution (time-symmetric) and measurement (irreversible). In standard quantum mechanics this asymmetry is imposed by the measurement postulate rather than derived.

Within VERSF, the asymmetry is structural:

- **Pre-temporal dynamics** in R are reversible because they involve no fact formation. Unitary operators on \mathcal{H} form a group under composition; every admissible transformation has an inverse.
- **Commitment events** via Φ are irreversible because they establish system–environment correlations that are redundantly distributed across a large number of uncontrolled environmental degrees of freedom. Reversing a commitment event would require a highly fine-tuned global recoherence operation acting on the entire joint system–environment state — not merely a local operation on the measured subsystem. Such an operation is not forbidden in principle by unitary quantum theory, but it is operationally inaccessible: once correlations have been dispersed into an uncontrolled environment with many degrees of freedom, no local or practical protocol can reassemble the coherence. This is the same mechanism invoked in quantum Darwinism and decoherence-based accounts of classical records — redundant environmental encoding makes reversal effectively impossible, and operationally corresponds to the thermodynamic irreversibility of macroscopic facts.

The **arrow of time** therefore emerges from the accumulation of commitment events: each Φ -triggered event adds an element to the ordered sequence of irreversible records in C that defines temporal succession. Physical time is the ordering relation induced by this sequence. Time-reversal symmetry holds within R ; it is broken only at Φ , where entropy-increasing commitment processes occur.

This resolves the measurement irreversibility problem without postulating time-reversal violation at the level of fundamental dynamics.

8. Comparison with Existing Interpretations

8.1 Copenhagen Interpretation

Copenhagen [15] treats wavefunction collapse as a rule for updating predictions upon measurement, not a physical process. VERSF agrees that the wavefunction describes pre-commitment possibilities rather than a distributed physical entity, but replaces Copenhagen's primitive collapse rule with a structured commitment criterion tied to entropy and causal

capacity, together with a stochastic outcome map Φ that specifies the conditions under which outcomes are registered. VERSF is a realist interpretation; Copenhagen is instrumentalist.

8.2 Many-Worlds Interpretation

Many-worlds [2] preserves unitary evolution universally by branching at each interaction, avoiding collapse entirely. The cost is an unexplained preferred basis (why do branches decompose in the pointer basis?) and a contested account of probability (why should branch weights equal Born probabilities?). VERSF avoids universal branching by providing an explicit commitment mechanism, and derives the Born rule from Gleason's theorem applied to the fold interface rather than requiring it as an additional postulate on branch weights.

8.3 Relational Quantum Mechanics

Rovelli's RQM [5] holds that quantum states are relative to observers: facts are relational events between systems. VERSF shares the relational emphasis — distinguishability relations in R are explicitly relational — and both frameworks treat facts as the basic units of physical reality. The key difference is temporal: RQM does not account for the *emergence* of time from fact formation. VERSF's pre-temporal layer provides a more fundamental account of why relational facts generate temporal structure, rather than presupposing a temporal framework within which relational facts occur.

8.4 QBism

QBism [6] treats quantum states as expressions of an agent's degrees of belief and measurement outcomes as personal experiences, dissolving the measurement problem by relocating it to the epistemic domain. This avoids the need for a physical collapse mechanism but at the cost of explicit ontological content: committed records in QBism are agent-relative, not mind-independent. VERSF is explicitly realist: committed records in C are objective, irreversible physical facts. The fold interface is a physical process, not an epistemic update.

8.5 Spontaneous Collapse Models (GRW/CSL)

Spontaneous collapse models [4] modify the Schrödinger equation with stochastic nonlinear terms causing spontaneous localisation at a rate $\lambda \sim 10^{-16} \text{ s}^{-1}$ per particle. This makes collapse a physical process — at the cost of a theoretically ad hoc parameter λ and a modified Schrödinger equation. VERSF retains the standard unitary Schrödinger equation in R and constrains the commitment threshold via the BCB framework rather than introducing a free parameter. The two frameworks make potentially distinguishable predictions in the mesoscopic regime: GRW predicts a mass-proportional collapse rate; VERSF predicts a commitment delay governed by the entropy threshold condition (Section 9).

9. Experimental Signatures and a Toy Model

A scientific interpretation of quantum mechanics must be distinguishable from alternatives in principle. We identify four experimental signatures. Sections 9.1 and 9.2 follow directly from the fold interface formalism developed here; Sections 9.3 and 9.4 follow from the substrate parameter triad established in companion VERSF work [17] and are reproduced here in the commitment-dynamics framework for consistency.

9.1 Commitment Delay in Mesoscopic Systems: Toy Model

The sharpest quantitative prediction of the present framework is $\tau_s \approx 0.28$ ps — the causal crossing time of the minimal commitment cell, fixed independently of any free parameter by $\tau_s = \xi/c$ and the single cosmological input ρ_Λ . This timescale governs the ultrafast switching crossover of Section 9.3 and requires no knowledge of S_{commit} . The following toy model demonstrates a *conditional* prediction that becomes quantitative once S_{commit} is fixed by the BCB framework.

Setup. Consider a system S with Hilbert space $\mathcal{H}_S = \mathbb{C}^2$, interacting with an N -mode bosonic environment E via a Jaynes–Cummings-type coupling:

$$H_{SE} = g \sum_{k=1}^N (\sigma_+ a_k + \sigma_- a_k^\dagger)$$

where σ_\pm are raising/lowering operators on S and a_k, a_k^\dagger are bosonic modes of E . Beginning in the product state $|+\rangle_S \otimes |\text{vac}\rangle_E$, the von Neumann entropy of the reduced state $\rho_S(t)$ grows as:

$$S(\rho_S(t)) \approx -\cos^2(g\sqrt{N}t) \log \cos^2(g\sqrt{N}t) - \sin^2(g\sqrt{N}t) \log \sin^2(g\sqrt{N}t)$$

in the single-excitation sector. $S = 0$ at $t = 0$ and reaches its maximum $\ln 2$ at $t = \pi/(2g\sqrt{N})$.

Decoherence onset. Standard decoherence theory predicts off-diagonal suppression on timescale $\tau_D \sim 1/(g\sqrt{N})$.

Conditional commitment time. Writing $S_{\text{commit}} = \alpha \ln 2$ for a dimensionless threshold parameter $\alpha \in (0, 1)$ — whose value is a prediction of the BCB framework not yet fixed within this paper — the commitment time is:

$$\tau_C = (1/(g\sqrt{N})) \arcsin(\sqrt{p_\alpha})$$

where p_α solves $-p_\alpha \log p_\alpha - (1 - p_\alpha) \log(1 - p_\alpha) = \alpha \ln 2$.

Conditional commitment delay. The delay between decoherence onset and commitment is:

$$\Delta\tau(\alpha) = \tau_C - \tau_D = (1/(g\sqrt{N}))(\arcsin(\sqrt{p_\alpha}) - 1)$$

For $\alpha \rightarrow 0$ (very low threshold), $\Delta\tau \rightarrow 0$ and commitment coincides with decoherence. For $\alpha \rightarrow 1$ (threshold near maximal entropy), $\Delta\tau \rightarrow \pi/(2g\sqrt{N}) - 1/(g\sqrt{N})$, which is positive and in principle measurable.

Status of this prediction. This is a conditional prediction: the scaling and existence of the delay are established by the toy model, but the precise magnitude depends on α , which requires a full BCB derivation of S_{commit} to fix. The toy model demonstrates that commitment-delayed-beyond-decoherence is a generic consequence of the entropy threshold structure, and that the delay grows with α . The sharpest present prediction — not conditional on α — is the $\tau_s \approx 0.28$ ps crossover of Section 9.3, which follows from ξ and c alone.

9.2 Non-Poissonian Timing Statistics Near Threshold

If the commitment threshold has a physical entropy scale S_{commit} , then for systems near the threshold, the distribution of commitment times is shaped by the stochastic fluctuations of $S(\rho_S(t))$ around S_{commit} . Standard decoherence predicts that measurement outcome probabilities are determined by the Born rule with no additional timing structure beyond Poissonian statistics. VERSF is consistent with non-Poissonian timing statistics for near-threshold systems, reflecting the discrete entropy structure of the threshold condition — but the sign and magnitude of any deviation depend on the functional form of $S(\rho_S(t))$ near S_{commit} and cannot be predicted without a BCB derivation of S_{commit} .

The present paper identifies non-Poissonian timing structure as a qualitative signature of threshold-triggered commitment, not a quantitative prediction. A rigorous prediction of the deviation's sign, magnitude, and dependence on detector architecture requires a quantitative model of threshold fluctuations beyond what the current BCB framework has yet provided. What can be said is that any systematic deviation from Poissonian timing statistics, in a regime where standard decoherence predicts none, would be qualitatively consistent with a threshold mechanism of this kind and would constitute evidence worth pursuing.

Such a signature could in principle be probed in precision photon-counting experiments or ion trap measurements where detection timing statistics can be resolved at sub-nanosecond scales with high repetition rates.

9.3 Ultrafast Switching and the τ_s Crossover

The substrate relaxation timescale $\tau_s \approx 0.28$ ps introduces a characteristic crossover in decoherence dynamics under ultrafast modulation of which-path coupling [17]. If which-path marking is switched on and off with a rise time Δt :

- For $\Delta t \ll \tau_s$: coherence loss lags or weakens relative to standard Markovian decoherence models, because the substrate has not had time to relax into a committed state. The visibility envelope recovers partially.
- For $\Delta t \gg \tau_s$: standard Markovian decoherence behaviour is recovered, because the substrate relaxes fully between switching events.

The crossover between these regimes occurs at $\Delta t \sim \tau_s \approx 0.28$ ps. This is a **non-Markovian signature** — the transient visibility envelope under ultrafast modulation will mis-match simple Markovian decoherence predictions for $\Delta t \lesssim \tau_s$.

Distinguishing VERSF from generic non-Markovian decoherence. A reviewer will rightly ask whether this is simply a standard environmental memory effect — many physical baths exhibit non-Markovian behaviour with characteristic correlation times. The VERSF prediction is differentiated in a specific way: the crossover timescale τ_s is not an environment-specific fit parameter. It is fixed independently by $\tau_s = \xi/c$, where ξ is the minimal commitment cell scale derived from the cosmological vacuum energy density. Crucially, τ_s is **cross-linked** to the Casimir deviation prediction of Section 9.4: any independent experimental refinement of ξ from Casimir measurements near $d \sim 82$ μm would correspondingly sharpen the predicted crossover timescale. This inter-prediction correlation — between an ultrafast quantum optics signature and a low-frequency Casimir measurement — is structurally distinctive and cannot arise from a conventional environmental memory effect, which has no connection to either ξ or the cosmological constant. The prediction is thus not "some finite memory time exists" but rather "the memory timescale is $\tau_s = \xi/c$, correlated with a specific mesoscopic Casimir deviation."

A further consequence: since $\tau_s = \xi/c$, any independent experimental refinement of ξ (e.g. from the Casimir measurement of Section 9.4) should produce a correspondingly refined prediction for the crossover timescale. The two signatures are therefore correlated, providing a cross-check on the substrate parameter triad.

This prediction is testable with ultrafast optical switching in entangled photon or atom interferometry experiments where pump-probe timing precision below 1 ps is achievable with current technology.

9.4 Casimir Force Deviation Near ξ

Companion VERSF work [17, 18] identifies the Casimir effect [23] as the most direct laboratory probe of the substrate coherence structure. The vacuum energy density at plate separation d scales as $\rho_{\text{Casimir}} \sim \hbar c/d^4$, which matches the substrate energy density $\rho_{\text{foam}} \sim \hbar c/\xi^4$ precisely when $d \approx \xi \approx 82$ μm . This scale-matching is not engineered: the coherence length ξ was fixed by the cosmological dark energy density, yet it coincides with the separation where Casimir physics intersects substrate physics.

Reference [18] identifies $d \approx \xi$ as the natural regime in which departures from standard vacuum-mode Casimir scaling first become plausible, as $\chi(L)$ approaches 1 and the substrate transitions from self-sustaining to vacuum-dominated. The modified Casimir energy takes the form:

$$E(L) = E_{\text{QED}}(L) \cdot f(L/\xi)$$

where $f(L/\xi) \rightarrow 1$ for $L \ll \xi$ and departs from unity as $L \rightarrow \xi$. The precise functional form of f requires the full VERSF substrate action, which is not yet available. However:

Sign of the expected deviation. Reference [18] argues for suppression rather than enhancement near ξ : as d approaches ξ from below, the substrate transitions toward the vacuum-dominated regime where fewer independent substrate modes can be maintained. If the total vacuum fluctuation density is partially replaced by the cosmological background rather than supplemented by it, the available mode density for Casimir summation decreases, producing a reduction in Casimir force. Reference [18] explicitly cautions that this is a *heuristic expectation*, not a derived prediction, pending the substrate-action calculation.

Order of magnitude. At $L = \xi/2 \approx 41 \mu\text{m}$, $\chi \approx 0.06$, suggesting the fractional deviation $|f - 1|$ may be of order a few percent at scales 40–80 μm , if the departure is gradual [18]. Reference [17] parameterises this as a Gaussian profile with peak deviation $\sim 1\%$ at $d \approx 85 \mu\text{m}$ and width $\sigma \sim 20 \mu\text{m}$; this phenomenological parameterisation provides an experimental target but should be understood as a minimal ansatz pending the microphysical derivation.

Falsifiability. The framework predicts some deviation in the vicinity of $d \sim \xi$, likely suppressive, with an estimated magnitude of order 1% near $d \approx 82 \mu\text{m}$, pending derivation of the full substrate action. The precise threshold for falsification cannot be stated independently of the derived functional form $f(L/\xi)$; the $\sim 0.3\%$ figure cited in [17] is tied to the Gaussian parameterisation and should be understood as an order-of-magnitude indicator rather than a rigorous falsifiability bound. What is falsifiable in principle is the existence of any systematic, reproducible deviation from standard Casimir scaling that peaks near $d \sim \xi$ and returns to standard behaviour away from it. The exact predicted profile and its sign are to be treated as provisional until the substrate action is computed.

The core experimental challenge is not raw force sensitivity — current Casimir experiments achieve precision at the 10^{-15} N level — but the extension of precision measurements into the 50–150 μm regime, where systematic errors from patch potentials, electrostatic offsets, and plate non-parallelism become dominant. A MEMS-based force sensor with laser interferometry for plate separation, scanning systematically through the predicted deviation region near ξ , represents the most direct test available with current technology. Complementary access may be possible via THz spectroscopy of vacuum fluctuations, since the coherence scale corresponds to $f_{\xi} = c/\xi \approx 3.66$ THz [18].

10. Discussion: Broader Implications

10.1 Classical Reality as Accumulated Commitment

The picture that emerges from VERSF is one in which classical reality is the accumulated record of irreversible commitment events. This aligns with Zurek's quantum Darwinism [16], in which classical objectivity arises from the redundant imprinting of information about a system's state across many environmental subsystems. In VERSF terms, quantum Darwinism describes the process by which $S(\rho_S)$ accumulates across multiple environmental modes, driving the system towards the commitment threshold through proliferation of environmental records.

10.2 Cosmological Implications

If commitment dynamics governed the formation of the first irreversible records in the early universe, the entropy threshold condition may have implications for early structure formation. This is a speculative direction, since quantum measurement theory does not straightforwardly couple to cosmological perturbation theory. We note only that if VERSF's commitment mechanism operated during the inflationary epoch, it may have influenced the transition from quantum fluctuations to classical density perturbations earlier or differently than standard decoherence-based accounts suggest. We leave this as a direction for future work requiring integration with VERSF's cosmological sector.

10.3 The Mesoscopic Quantum Boundary

Reference [20] identifies a suggestive empirical coincidence between ξ and scales relevant to the quantum–classical transition in laboratory systems. Environmental decoherence correlation lengths in realistic laboratory conditions — gas collisions, thermal radiation, phonon environments — span approximately $10^{-6} - 10^{-4}$ m, a range that brackets ξ from below. The mesoscopic regime, in which environmental decoherence becomes competitive with coherent quantum evolution, has its characteristic upper boundary near $100 \mu\text{m}$. The scale $\xi \approx 82 \mu\text{m}$ sits within this range.

This numerical proximity is notable, but the framing requires care. The relevant scale for quantum interference is the de Broglie wavelength of the system, not its physical size; large molecules demonstrating interference have nanometre de Broglie wavelengths despite micrometre physical extents. The coincidence should therefore be understood as follows: the decoherence correlation lengths set by realistic environments bracket ξ from below, suggesting that ξ marks a substrate-level threshold in the same regime where environmental decoherence becomes dominant. This is a structural alignment — both descriptions concern the onset of irreversible entropy production at a characteristic causal scale — but it is not a quantitative prediction of specific laboratory decoherence rates, which depend on detailed environmental parameters not modelled within the current VERSF framework.

Reference [20] notes that the physical content of both descriptions is closely aligned: decoherence occurs when environmental interactions generate irreversible entropy production, and the $\chi(L) \sim 1$ threshold marks precisely the scale at which a causal region first becomes capable of supporting irreversible physical events within its own causal boundary. The VERSF framework and decoherence theory may characterise closely related aspects of the same transition — the onset of irreversible entropy production at a characteristic causal scale — with the stratification:

Scale	Expected behaviour
$L \ll \xi$	Predominantly reversible quantum evolution
$L \sim \xi$	Onset of irreversible classical record formation
$L \gg \xi$	Classical world dominates

This structural alignment is more than numerical: the ingredients of both descriptions — causal crossing time, quantum action, entropy production, distinguishable state transitions — are the same. A full derivation of standard decoherence scales from within the VERSF framework is not yet available and remains a priority for future work.

10.4 Cross-Scale Hierarchy and the χ Invariant

Reference [20] demonstrates that $\chi(L)$ yields structurally consistent results across 120 orders of magnitude:

Scale	$\chi(L)$	Physical interpretation
Planck length L_P	~ 1	Quantum gravity threshold
VERSF coherence scale ξ	$= 1$	First classical record formation (present epoch)
Schwarzschild horizon R	$\sim R^2/L_P^2$	Bekenstein–Hawking entropy S_{BH}
Cosmological horizon R_H	$\sim 10^{122}$	Total universe causal capacity

The same invariant spanning this range in a structurally consistent way — reproducing the Bekenstein–Hawking entropy at black hole horizons (supported by Bousso's covariant entropy bound [26] and Jacobson's thermodynamic derivation of general relativity [21]), and coinciding with Lloyd's estimate of the universe's total computational capacity at the cosmological horizon [27] — is what distinguishes a fundamental capacity measure from a dimensional coincidence [20]. The entropic gravity approach of Verlinde [22] offers a complementary perspective: in that framework gravity itself emerges from entropy gradients at horizons, a thermodynamic structure consistent with the $\chi(L)$ picture in which the quartic capacity measure underlies both the emergence of gravitational dynamics and the formation of irreversible classical records.

The VERSF coherence scale ξ sits at the lower end of this hierarchy as the threshold at which the vacuum energy density of the present cosmological epoch first becomes capable of classical fact formation. The era coherence scale picture [18] generalises this: each cosmic epoch has a characteristic commitment scale $L_i = (\hbar c/\rho_i)^{1/4}$, and the current epoch's value is ξ .

Quartic capacity and area scaling. A potential confusion warrants clarification. The quartic capacity parameter $\chi(L)$ scales as L^4 — equivalently as volume \times time. Realised classical information, however, is bounded by boundary correlations and therefore scales with area (L^2) rather than volume, consistent with holographic entropy bounds. These two scalings coexist without contradiction: $\chi(L)$ measures the total action budget available to a causal region over its crossing time — a dynamical *process capacity* measuring how much can happen, not how much can be stored — while realised classical information measures stable classical storage capacity, which is constrained by the area of the bounding surface. To be explicit: $\chi(L)$ is not an entropy-storage law. It is a causal throughput measure that quantifies the rate of irreversible event production within a bounded region. The distinction is between what a region *can do* dynamically (quartic) and what it *stably encodes* as classical information (area). The commitment threshold $\chi \sim 1$ governs the onset of process capacity; the holographic bound governs the maximum stable classical record density.

11. Conclusion

Wave–particle duality within the VERSF framework is not a fundamental contradiction but a reflection of two stages in the formation of physical facts. The key results of this paper are:

1. **The VERSF axioms imply a complex Hilbert representation.** Following the established Hardy–CDP reconstruction programmes [7, 8], the full derivation chain — operational distinguishability → convex state space → compact transitive Lie group action → elimination of \mathbb{R} and \mathbb{H} on grounds of tomographic locality and composite system consistency — implies that the state space must admit a complex Hilbert representation. VERSF's contribution is grounding these axioms in the commitment ontology of pre-temporal relational space rather than treating them as free-standing operational postulates.
2. **The Schrödinger equation describes pre-temporal dynamics.** Unitary evolution in \mathcal{H} is the evolution of commitment pathway amplitudes in R , where physical time is not yet defined.
3. **The Born rule emerges from Gleason's theorem.** The requirement that $\Phi : \mathcal{H} \rightarrow \mathcal{P}$ define a consistent probability measure over committed outcomes uniquely fixes the Born rule for $\dim \mathcal{H} \geq 3$.
4. **The fold interface is mathematically defined and universally grounded.** Φ is a stochastic outcome map triggered when the von Neumann entropy $S(\rho_S) \geq S_{\text{commit}}$ of the system–environment reduced state. The commitment threshold S_{commit} is linked to the causal capacity condition $\chi(\xi) = \rho_{\Delta} \xi^4 / (\hbar c) = 1$ through the Bekenstein entropy bound: both conditions express the minimum entropic capacity required for one irreversible record, though they arise from different domains (entanglement entropy vs causal geometry).

Open problem. The precise formal equivalence of the S_{commit} threshold and the $\chi \sim 1$ condition within a single VERSF microscopic framework remains to be derived. This is identified as a priority for the BCB programme.

Papers [19, 20] establish that $\chi(L)$ is a *universal* invariant arising independently from quantum mechanics (Margolus–Levitin), thermodynamics (Bekenstein), causal geometry (diamond action), and information theory (Lloyd computational bound). The threshold $\chi \sim 1$ is where the quantum speed limit, thermodynamic entropy capacity limit, and computational capacity limit all coincide simultaneously. VERSF's specific contribution is identifying $\rho = \rho_{\Delta}$ as the relevant energy density; the quartic structure and the threshold are universal physics structurally consistent across scales spanning roughly 120 orders of magnitude [20].

5. **Wave behaviour is possibility propagation.** Interference arises from the interaction of possible commitment pathways in R before any irreversible record is produced.
6. **Particle detection is commitment.** A localised detection event corresponds to an irreversible crossing of Φ , producing a physical record in C .

7. **The arrow of time is derived.** Time-reversal symmetry holds in R ; it is broken only at Φ , where entropy-increasing commitment events generate the ordered sequence of facts constituting physical time.
8. **VERSF identifies four experimentally accessible signatures.** The commitment delay $\Delta\tau$ in mesoscopic systems (Section 9.1), non-Poissonian timing statistics near threshold (Section 9.2), the $\tau_s \approx 0.28$ ps crossover in ultrafast switching experiments (Section 9.3), and a predicted departure from standard Casimir scaling near $d \approx \xi \approx 82 \mu\text{m}$ (Section 9.4) are all in principle observable with current or near-future technology. The Casimir functional form $f(L/\xi)$ and its sign are heuristic expectations pending derivation of the full substrate action [18]; the $\sim 1\%$ parameterisation of [17] provides an experimental target while the microphysical derivation is in progress.

In this way, spatial coherence domains in committed spacetime act as the physical environments within which reversible relational dynamics can unfold before the entropy threshold for commitment is reached. Their scale $\xi \approx 82 \mu\text{m}$ is not a fundamental constant of R but the size of the minimal commitment cell — the smallest region of committed spacetime C capable of producing one irreversible record within its own causal horizon, fixed by $\chi(\xi) = 1$ and derivable from \hbar , c , and ρ_Λ alone [18].

Wave–particle duality therefore reflects the boundary between possibility and reality: the continuous process by which the universe converts potential configurations within pre-temporal relational space into irreversible facts that generate the flow of time.

References

- [1] Bell, J. S. (1990). Against 'measurement'. *Physics World*, 3(8), 33–40.
- [2] Everett, H. (1957). "Relative state" formulation of quantum mechanics. *Reviews of Modern Physics*, 29(3), 454–462.
- [3] Bohm, D. (1952). A suggested interpretation of the quantum theory in terms of "hidden" variables. *Physical Review*, 85(2), 166–179.
- [4] Ghirardi, G. C., Rimini, A., & Weber, T. (1986). Unified dynamics for microscopic and macroscopic systems. *Physical Review D*, 34(2), 470–491.
- [5] Rovelli, C. (1996). Relational quantum mechanics. *International Journal of Theoretical Physics*, 35(8), 1637–1678.
- [6] Fuchs, C. A., Mermin, N. D., & Schack, R. (2014). An introduction to QBism with an application to the locality of quantum mechanics. *American Journal of Physics*, 82(8), 749–754.
- [7] Hardy, L. (2001). Quantum theory from five reasonable axioms. arXiv:quant-ph/0101012.

- [8] Chiribella, G., D'Ariano, G. M., & Perinotti, P. (2011). Informational derivation of quantum theory. *Physical Review A*, 84(1), 012311.
- [9] Borel, A. (1949). Some remarks about Lie groups transitive on spheres and tori. *Bulletin of the American Mathematical Society*, 55(6), 580–587.
- [10] Adler, S. L. (1995). *Quaternionic Quantum Mechanics and Quantum Fields*. Oxford University Press.
- [11] Landauer, R. (1961). Irreversibility and heat generation in the computing process. *IBM Journal of Research and Development*, 5(3), 183–191.
- [12] Zurek, W. H. (2003). Decoherence, einselection, and the quantum origins of the classical. *Reviews of Modern Physics*, 75(3), 715–775.
- [13] Gleason, A. M. (1957). Measures on the closed subspaces of a Hilbert space. *Journal of Mathematics and Mechanics*, 6(6), 885–893.
- [14] Deutsch, D. (1999). Quantum theory of probability and decisions. *Proceedings of the Royal Society A*, 455(1988), 3129–3137.
- [15] Bohr, N. (1928). The quantum postulate and the recent development of atomic theory. *Nature*, 121, 580–590.
- [16] Zurek, W. H. (2009). Quantum Darwinism. *Nature Physics*, 5(3), 181–188.
- [17] VERSF Theoretical Physics Program, AIDA Institute (2025). When space itself has mass: What we learned from the double-slit experiment. VERSF Working Paper.
- [18] VERSF Theoretical Physics Program, AIDA Institute (2025). The spacetime coherence length: Vacuum-energy crossover, information throughput, and scale hierarchy in the VERSF framework. VERSF Working Paper.
- [19] VERSF Theoretical Physics Program, AIDA Institute (2025). The quartic capacity of causal regions: Why energy density, action, entropy, and information throughput converge on ρL^4 . VERSF Working Paper.
- [20] VERSF Theoretical Physics Program, AIDA Institute (2025). From quantum speed limits to cosmological horizons: The quartic capacity parameter of bounded spacetime regions. VERSF Working Paper.
- [21] Jacobson, T. (1995). Thermodynamics of spacetime: The Einstein equation of state. *Physical Review Letters*, 75(7), 1260–1263.
- [22] Verlinde, E. (2011). On the origin of gravity and the laws of Newton. *Journal of High Energy Physics*, 2011(4), 29.

- [23] Casimir, H. B. G. (1948). On the attraction between two perfectly conducting plates. *Proceedings of the Royal Netherlands Academy of Arts and Sciences*, 51, 793–795.
- [24] Margolus, N. & Levitin, L. B. (1998). The maximum speed of dynamical evolution. *Physica D*, 120, 188–195.
- [25] Bekenstein, J. D. (1981). Universal upper bound on the entropy-to-energy ratio for bounded systems. *Physical Review D*, 23, 287–298.
- [26] Bousso, R. (1999). A covariant entropy conjecture. *Journal of High Energy Physics*, 07, 004.
- [27] Lloyd, S. (2000). Ultimate physical limits to computation. *Nature*, 406, 1047–1054.
- [28] VERSF Theoretical Physics Program, AIDA Institute (2025). The Fold Interface Law: Structural derivation of the commitment boundary between reversible relational space and committed spacetime. VERSF Working Paper.
-

Appendix A: Summary for General Readers

Quantum mechanics contains one of the strangest puzzles in all of science: the same object — an electron, a photon — can behave like a spread-out wave or like a tiny localised particle, depending on how you look at it. Fire electrons one at a time at a barrier with two slits, and over time they build up an interference pattern on the screen behind it, as if each electron passed through both slits simultaneously like a wave. Yet every individual electron lands at a single point on the screen, as if it were a particle. How can the same thing be both at once?

Standard physics describes this with a mathematical object called the wavefunction, which evolves smoothly like a wave until a measurement is made — at which point it "collapses" to a definite outcome. But what physically causes this collapse? That question has been debated for a century without a settled answer.

This paper proposes a new answer rooted in the Void Energy-Regulated Space Framework (VERSF). The key idea is that physical reality has two layers. The first is a **pre-temporal relational space** — a domain of reversible possibilities that has not yet generated any facts or any physical time. The second is **committed physical reality** — the layer of irreversible records that makes up the observable universe and from which time itself emerges.

In this picture, the wave behaviour of a quantum particle corresponds to the exploration of possible outcomes within the first layer: no fact has yet been formed, so all possibilities coexist and interfere with one another. Particle behaviour — the sharp click of a detector — corresponds to a **commitment event**: the moment when one possibility crosses a threshold and becomes an irreversible physical record. That threshold is defined by a precise condition: commitment happens when the particle's entanglement with its environment has grown large enough — and

persisted long enough — that an irreversible record can be completed within the region's own causal boundary. Companion VERSF work establishes that the smallest region capable of doing this has a characteristic size of roughly 10^{-4} m — about the width of a human hair — derived entirely from the measured energy density of empty space.

Wave–particle duality, in this view, reflects two phases of the same fact-formation process: reversible possibility propagation within the pre-temporal layer, and irreversible commitment at the fold interface.

What makes this particularly powerful is that the threshold for commitment is not invented by VERSF. It is a universal result arising independently from quantum mechanics, thermodynamics, and the causal geometry of spacetime. The quantum speed limit and the thermodynamic entropy capacity both independently point to the same threshold. VERSF's specific contribution is identifying the cosmological vacuum energy density as the relevant energy scale, which fixes the minimal commitment cell at roughly 10^{-4} m. When this threshold is reached, the fold interface converts reversible relational amplitudes into irreversible physical records.

The paper shows that this framework is not just a philosophical reinterpretation. The structure of quantum mechanics — including why probabilities work the way they do — follows as a logical consequence of the VERSF axioms. The framework also makes predictions that differ, in principle, from standard quantum mechanics, and identifies experiments that could test those differences.

Appendix B: Derivation of the Quartic Capacity Measure $\chi(L)$

This appendix provides a self-contained derivation of the quartic causal-capacity parameter $\chi(L) = \rho L^4 / (\hbar c)$, making explicit the minimal reasoning required in the present paper. The purpose is not to replace the fuller treatment in companion work [19, 20], but to establish that the derivation is self-contained and does not rely on inaccessible manuscripts.

B.1 Motivation

The central question is: what dimensionless quantity measures the capacity of a bounded causal region to support irreversible physical events?

Consider a region of characteristic linear size L , mean energy density ρ , and causal crossing time:

$$T(L) \sim L/c$$

If irreversible record formation requires a minimum action cost of order \hbar per distinguishable event, then the natural quantity is the total action available within the region over one causal crossing time, divided by \hbar .

The total energy contained in the region scales as $E(L) \sim \rho L^3$. Over the causal time $T(L) \sim L/c$, the total available action is:

$$\mathcal{S}(L) \sim E(L) \cdot T(L) \sim \rho L^3 \cdot (L/c) = \rho L^4/c$$

Dividing by the quantum of action gives the dimensionless ratio:

$$\chi(L) \equiv \mathcal{S}(L)/\hbar \sim \rho L^4/(\hbar c)$$

This is the quartic capacity measure used throughout the paper. Its physical interpretation is immediate: $\chi(L)$ is the number of elementary action quanta available to a causal region of size L over its own light-crossing time. When $\chi(L) \ll 1$, the region is under-capacitated for irreversible record formation; when $\chi(L) \sim 1$, it reaches the threshold for a single distinguishable irreversible event; when $\chi(L) \gg 1$, it supports many such events.

B.2 Dimensional Uniqueness

It is useful to show that the quartic structure is not arbitrary. Before proceeding, two scope clarifications are necessary.

Why restrict to monomials? The argument below shows that any dimensionless monomial in (ρ, L, \hbar, c) must take the quartic form. One could in principle consider non-monomial combinations such as $\rho L^4/(\hbar c) + (\rho L^4/(\hbar c))^2$. However, the leading-order threshold is determined by the monomial alone: near $\chi \sim 1$, higher-order terms are subdominant for $\chi < 1$ and the physical threshold condition is set by the first term regardless of such corrections.

Why exclude G? Both primary derivations — the Margolus–Levitin quantum throughput argument and the Bekenstein entropy bound — make no reference to gravity. The ML bound is a purely quantum-mechanical result; the Bekenstein bound is derived from thermodynamics and quantum theory without invoking the gravitational coupling constant. The variable set (ρ, L, \hbar, c) without G is therefore the correct starting point for a capacity measure grounded in these two derivations. Including G would introduce gravitational physics that neither primary derivation requires, overstating the generality of the quartic. (As noted in Section 10.4, the quartic capacity does extend consistently to gravitational contexts at black hole and cosmological horizons, but that is a structural validation, not a derivation; the primary result stands without G .)

With this scope established: suppose one seeks a dimensionless monomial built only from ρ, L, \hbar , and c :

$$X = \rho^a L^b \hbar^d c^e$$

Using SI dimensions $[\rho] = M L^{-1} T^{-2}$, $[L] = L$, $[\hbar] = M L^2 T^{-1}$, $[c] = L T^{-1}$, demanding X be dimensionless gives the system:

$$a + d = 0 \quad -a + b + 2d + e = 0 \quad -2a - d - e = 0$$

From the first equation $d = -a$; from the third $e = -a$; substituting into the second gives $b = 4a$. Hence every dimensionless monomial built from (ρ, L, \hbar, c) alone must be of the form:

$$X = (\rho L^4 / (\hbar c))^a$$

The unique dimensionless monomial (up to overall power) is therefore $\rho L^4 / (\hbar c)$. Combined with the scope clarifications above, this establishes that the quartic is not inserted by hand: it is the unique dimensionless capacity ratio available from the physically appropriate variable set, and the threshold condition at $\chi \sim 1$ is robust to higher-order terms.

B.3 Two Genuinely Independent Physical Routes

The quartic expression is supported by two independent physical arguments.

B.3.1 Quantum throughput route. A region of energy $E \sim \rho L^3$ can undergo at most a finite number of distinguishable transitions in time T . The Margolus–Levitin bound [24] implies:

$$N_{ML} \lesssim ET/\hbar$$

Setting $T \sim L/c$ gives $N_{ML} \sim \rho L^4 / (\hbar c) = \chi(L)$. So $\chi(L)$ measures the maximum number of distinguishable quantum updates within one causal crossing time.

B.3.2 Entropy-capacity route. For a bounded region of radius L and energy $E \sim \rho L^3$, the Bekenstein entropy bound [25] gives:

$$S_{max} \lesssim EL/(\hbar c)$$

Substituting $E \sim \rho L^3$ yields $S_{max}(L) \sim \rho L^4 / (\hbar c) = \chi(L)$. So $\chi(L)$ also measures the maximum entropy capacity of the region.

These two routes are logically distinct: the first is a quantum speed-limit argument concerning distinguishable state evolution; the second is a thermodynamic bound on entropy content. Their convergence on the same quartic structure is therefore non-trivial.

B.4 Reformulations

Two additional expressions are useful, though they are reformulations rather than logically independent derivations.

The action of a causal diamond of size L scales as $\mathcal{S} \diamond \sim \rho L^4 / c$, so $\mathcal{S} \diamond / \hbar \sim \chi(L)$. Lloyd's bound [27] on computational operations in time T is also proportional to ET/\hbar , and therefore reproduces

$\chi(L)$ when $E \sim \rho L^3$ and $T \sim L/c$. This is best viewed as a computational reformulation of the same capacity measure.

B.5 Why $\chi(L) \sim 1$ is the Threshold

The condition $\chi(L) \sim 1$ marks the point at which all interpretations above reach the same minimal threshold simultaneously:

- one quantum of available action
- one distinguishable transition over a causal crossing time
- one bit-scale entropy capacity
- one logical update in computational language

This is why $\chi(L) = 1$ is the threshold for minimal irreversible record formation.

B.6 VERSF-Specific Identification

Up to this point no specifically VERSF assumption has been made beyond taking seriously the physical relevance of bounded causal regions and irreversible record formation. The specifically VERSF step is the identification $\rho = \rho_\Lambda$, where ρ_Λ is the cosmological vacuum energy density. Once this identification is made, the quartic threshold condition $\chi(L) = \rho_\Lambda L^4/(\hbar c) = 1$ determines a unique coherence scale $\xi = (\hbar c/\rho_\Lambda)^{1/4}$, which is established in Appendix C.

Appendix C: Minimal Commitment Cell Lemma

This appendix states and proves the Minimal Commitment Cell Lemma used in the main text.

C.1 Statement

Lemma. Let a bounded causal region of characteristic size L have mean substrate energy density ρ , and suppose that irreversible fact formation requires, within one causal crossing time, at least one quantum of action, one distinguishable state transition, and one bit-equivalent entropy capacity. Then the minimal scale at which these conditions become simultaneously achievable is the unique solution of:

$$\chi(L) = \rho L^4/(\hbar c) = 1$$

For the present cosmological vacuum, $\rho = \rho_\Lambda$, this scale is:

$$\xi = (\hbar c/\rho_\Lambda)^{1/4}$$

This scale defines the **minimal commitment cell**.

C.2 Proof by Simultaneous Threshold Matching

From Appendix B, $\chi(L)$ simultaneously measures:

$$\chi(L) \sim \mathcal{S}(L)/\hbar \sim N_{\text{ML}} \sim S_{\text{max}}(L)$$

up to order-unity geometric coefficients.

Imposing the minimal requirement for a region to support one irreversible record within its own causal domain — $\mathcal{S}(L) \gtrsim \hbar$, $N_{\text{ML}} \gtrsim 1$, $S_{\text{max}}(L) \gtrsim k_{\text{B}} \ln 2$ — all three conditions reduce to the same threshold:

$$\chi(L) \sim 1$$

Solving $\rho L^4/(\hbar c) = 1$ gives $L = (\hbar c/\rho)^{1/4}$. Specialising to $\rho = \rho_{\Lambda}$ yields $\xi = (\hbar c/\rho_{\Lambda})^{1/4}$. This establishes existence.

For minimality: since $\chi(L) = \rho_{\Lambda} L^4/(\hbar c)$ is strictly monotonically increasing in L , the equation $\chi(L) = 1$ has a unique solution ξ , which is therefore the unique minimal scale satisfying the commitment criterion. For $L < \xi$, then $\chi(L) < 1$ and the region fails all three threshold requirements simultaneously — it contains less than one quantum of effective causal action, cannot support one distinguishable update per crossing time, and has insufficient entropy capacity for a single minimal record. For $L > \xi$, then $\chi(L) > 1$ and the region is supercritical but no longer minimal. Therefore $L = \xi$ is the unique minimal commitment scale.

C.3 Numerical Value

From $\hbar \approx 1.055 \times 10^{-34}$ J s, $c \approx 2.998 \times 10^8$ m s⁻¹, $\rho_{\Lambda} \approx 6.9 \times 10^{-10}$ J m⁻³:

$$\xi = (\hbar c/\rho_{\Lambda})^{1/4} \approx 8.2 \times 10^{-5} \text{ m} \approx 82 \text{ } \mu\text{m}$$

C.4 Associated Substrate Scales

Once ξ is fixed, the associated substrate timescale and inertial scale follow immediately:

$$\tau_s = \xi/c \approx (8.2 \times 10^{-5})/(2.998 \times 10^8) \approx 2.7 \times 10^{-13} \text{ s} \approx 0.28 \text{ ps}$$

$$m_s = \hbar/(c\xi) \approx 4 \times 10^{-39} \text{ kg}$$

These three quantities (ξ , τ_s , m_s) form the **substrate parameter triad** referenced throughout the paper.

C.5 Why the Cell is a Commitment Cell

The scale ξ is not merely a correlation length or phenomenological crossover. It is the smallest region for which the following hold together: sufficient action for one irreversible update,

sufficient causal time for that update to complete internally, and sufficient entropy capacity for one record. Below this scale, reversible possibility propagation may occur, but the region is under-capacitated for autonomous commitment. At and above this scale, record formation becomes causally self-sustaining.

C.6 Relation to Friedmann Cosmology

Writing the vacuum energy density via the Friedmann equation $\rho_{\Lambda} = 3H_0^2/(8\pi G)$ and substituting into the definition of ξ :

$$\xi = (\hbar c/\rho_{\Lambda})^{1/4} = (8\pi G\hbar c/(3H_0^2))^{1/4}$$

Using $L_P = (\hbar G/c^3)^{1/2}$, this simplifies to:

$$\xi = (8\pi/3)^{1/4} \cdot \sqrt{L_P \cdot c/H_0}$$

This relation is not inserted by hand — it follows directly from combining the quartic threshold condition with the Friedmann relation. ξ is the geometric mean, up to the order-unity coefficient $(8\pi/3)^{1/4} \approx 1.70$, of the Planck length and the Hubble radius.

C.7 Scope

The lemma establishes the minimal commitment scale within the present causal-capacity construction. It does not imply that every manifestation of decoherence in laboratory systems occurs at exactly ξ , nor that ξ replaces conventional environmental decoherence scales. Rather, it shows that ξ is the minimal substrate-defined scale at which irreversible record formation becomes causally self-sustaining in a vacuum-dominated spacetime. This is the precise sense in which ξ functions as the minimal commitment cell in the VERSF framework.